

# EJECTED BEAM EMITTANCE OF THE SPRING-8 BOOSTER SYNCHROTRON

K. Fukami, T. Aoki, T. Asaka, N. Hosoda, T. Nakazato, T. Ohshima, S. Sasaki, M. Shoji,  
H. Yonehara and C. Zhang

SPring-8, 1-1-1, Kouto, Mikuzuki-cho, Sayo-gun, Hyogo, 679-5198, JAPAN

## Abstract

In order to estimate an energy dependence of the electron beam emittance of the SPring-8 booster synchrotron, six optical transition radiation monitors were installed along the ejected beam-dump line. We measured the emittance with the energy from 3 GeV to 8 GeV. Horizontal emittances were measured to be  $32 \pm 5$  nrad and  $200 \pm 29$  nrad at the energy of 3 GeV and 8 GeV, respectively. In horizontal direction, emittance growth by the intra-beam scattering was not observed at this energy region.

## 1 INTRODUCTION

The SPring-8 booster synchrotron accepts an electron beam with the energy of 1 GeV from the linac. The beam is accelerated up to 8 GeV and then ejected to stack into the storage ring [1]. The synchrotron consists of a FODO lattice of 40 cells and its circumference is 396.124 m. There are 64 bending, 80 quadrupole, 60 sextupole and 80 correction magnets. The beam energy is kept constant in the injection with a period of about 250 ms (flat-bottom). Then, it is increased linearly in the energy-ramping at about 350 ms and is kept constant in the ejection at about 130 ms (flat-top).

As a low-energy operation of the storage ring has been planned and tested, the synchrotron is required to lower its ejection energy. Matching between an acceptance of the storage ring and an emittance of the synchrotron is important. In this paper, we report an energy dependence of the emittance of the ejected beam. Although emittance-measurements with a wire scanner were reported by several facilities [2], we introduced an optical transition radiation (OTR) monitor. We had to measure the beam size shot by shot because the change in beam position was not small enough at low energies to measure the beam size with the wire monitor.

## 2 INSTRUMENTATION

In a dispersion-free drift-space, the beam size  $\sigma_s$  [m] at the distance  $L$  [m] downstream from a quadrupole magnet with the integrated strength of  $k$  [ $m^{-1}$ ] is written as

$$\sigma_s^2 = \varepsilon \{ (k^2 \beta_Q - 2k\alpha_Q + \gamma_Q)L^2 + 2(k\beta_Q - \alpha_Q)L + \beta_Q \}$$

$$\equiv A(L - B)^2 + C, \quad (1)$$

where  $\varepsilon$  [mrad] is the emittance,  $\alpha_Q$ ,  $\beta_Q$  [m] and  $\gamma_Q$  [ $m^{-1}$ ]

are the Twiss-parameters at the position of the quadrupole magnet. By using the coefficients  $A$  and  $C$ , the emittance is expressed by

$$\varepsilon = \sqrt{AC}. \quad (2)$$

The OTR is generated when a charged particle crosses the interface of two media with different dielectric constants, in both backward and forward directions [3,4]. We installed six OTR monitors at the same intervals of 2.65 m along the beam-dump line (Fig.1). The OTR was generated using an aluminum plate (OTR plate), whose surface roughness was less than 5  $\mu m$ . One of the OTR plate, a scaling plate, or no plate (blank) is selected and set on the beam line by the three-position actuator (Fig.2). The scaling plate was used to calibrate the OTR image. The plate was illuminated by LEDs, which was placed surrounding the lower view port. The positioning error of the center of each plate was less than 0.1 mm.

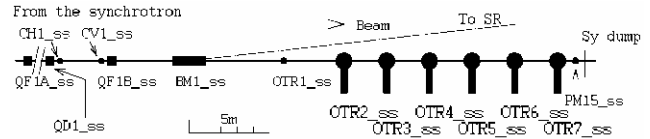


Figure 1: Arrangement of the OTR-monitors and the beam-dump line. From the side of upstream, six monitors were named in order of OTR2\_ss - OTR7\_ss.

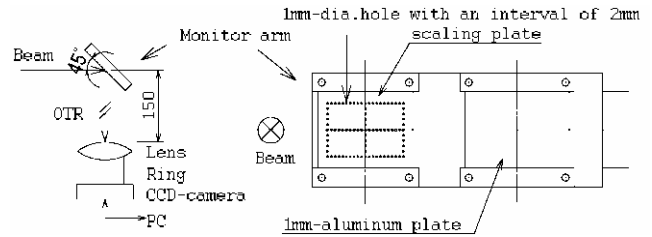


Figure 2: Detail of the OTR monitor. Left side figure shows position relation between a monitor arm and a CCD-camera. Right side figure shows the scaling plate and the OTR plate.

Images of the plates were observed using a 2/3" CCD-camera (Pulnix Inc., TM-1320-15CL, 1296 x 1018 pixels, 8 bits resolution). To magnify the image, 40-mm long close-up ring was inserted between the camera and lens (CANON Inc., VF75-1.8). At the position of the lens, divergences of the OTR at the energy of 3 GeV and 8 GeV are estimated to be 17 and 6  $\mu m$ , respectively [4]. The lens-caliber ( $\phi 48$ ) is much larger than the divergence.

The image was digitized and was transferred to a PC by a camera-link cable.

Horizontal and vertical scales were calibrated to be  $11.6 \pm 0.9 \mu\text{m}/\text{pixel}$  by using the scaling plate for all monitors. The error caused by an inaccuracy of the scaling plate is much smaller than the error above.

### 3 MEASUREMENT

The ejected beam energy was selected from 3 GeV to 8 GeV with 1-GeV step. Ejected energy was changed by scaling the excitation current of all the magnets during the flat-top period. The RF acceleration voltage was set to the value of 18 MV for the energy of 8 GeV and was set in proportional to the beam energy. An effect caused by this condition is discussed below. For all energies, strengths of the focusing-quadrupole magnets of QF1A<sub>ss</sub> and QF1B<sub>ss</sub> (see Fig.1) were adjusted so that the minimum point of horizontal beam size (waist) might come to the position of OTR4<sub>ss</sub>.

One of six OTR-plates was inserted during one measurement. From the linac, electrons were injected only one bunch of the synchrotron. The beam intensity was set to be  $5.8 \times 10^9$  electrons/bunch, which was equivalent to the averaged beam current of 0.7 mA. The CCD camera was synchronized with the beam-ejection signal. Exposure time of it was set to be 1/125 sec. The kicking angles of horizontal (CH1<sub>ss</sub>) and vertical (CV1<sub>ss</sub>) steering magnets (see Fig.1) were adjusted to center the beam position at each monitor. Ten images were captured every condition to carry out statistics analysis.

### 4 EXPERIMENTAL RESULTS

Background images were measured under the condition of no beam. There were subtracted from the raw image. The OTR image had an elliptical shape with a major axis in horizontal direction. The axes had a rotation from the alignment axes (x and y). The rotation angles were estimated from the correlation coefficients of the distributions, and its maximum angle was  $-38$  mrad for the OTR7<sub>ss</sub> at the energy of 7 GeV. It is considered that this rotation is caused by the following two reasons. One is a setting error of the camera, which is designed less than 20 mrad. The other is vertical dispersion. The rotation angle corresponds to the ratio of the vertical dispersion to the horizontal one. Both of them are the same order as the axes rotation.

In order to estimate the emittance, we introduced a virtual pixel coordinate system. The major axis and minor axis of the beam ellipse were newly defined as X- and Y-axis. An origin of these axes was selected at the position of the beam-center. The virtual pixels were located a mesh parallel to the X-Y axes with the same pixel size as the camera. Intensities at the virtual pixels were determined by the interpolation from neighboring-four real pixel data. The data of the virtual pixels were integrated and projected to the X-Y axes. An example of the distribution of the OTR4<sub>ss</sub> at the energy

of 8 GeV is shown in Fig.3. We assumed that the beam intensity distribution had a gaussian shape. The beam size was defined as one standard deviation of the gaussian.

In the horizontal data, an excessive intensity was piled up at right side of the figure. It may be cause by a synchrotron radiation from the magnets at the upstream of the dump line. To check this phenomenon, an image was captured when the beam was deflected so that the beam did not hit the OTR-plate using the CV1<sub>ss</sub> (see red-dot in Fig.3). Measured intensity agreed with the excessive intensity in the right side of the figure.

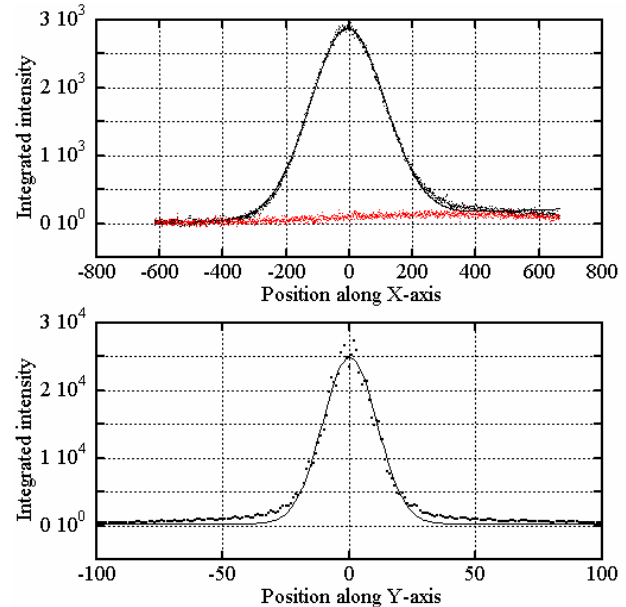


Figure 3: Upper and lower figure show integrated intensity in horizontal and vertical directions of the OTR4<sub>ss</sub> at the energy of 8 GeV, respectively. Lines indicate results of the gaussian-fit. Red-dot indicates the intensity due to a synchrotron radiation.

We assumed that the intensity due to the synchrotron radiation was linear to the X- and Y-axes. Hence, a least-squares method was performed with a following function,

$$I_Z = a_1 \text{Exp}\left[-\frac{1}{2} \frac{(Z - a_2)^2}{\sigma_Z^2}\right] + a_3 + a_4 Z, \quad (3)$$

where, Z indicates X or Y, I is the intensity,  $\sigma$  is the beam size and  $a_i$  ( $i=1,2,\dots,4$ ) are coefficients. For all monitors and all ejected energies, the same analysis was performed.

A standard deviation of the ten measurements of the beam size was so large at low energy. The deviation of the horizontal beam sizes at the energy of 8 GeV and 3 GeV were 0.2 % and 2 %, respectively. An error of the beam size was estimated by the root-mean-square of the above ratio and the error of scale.

The horizontal beam size is not decided only by  $\epsilon\beta$  (emittance-term in this paper) in the dump-line because the line is not dispersion-free. Therefore, by using a designed dispersion and a natural energy-spread, the beam size due to the dispersion was subtracted from

the measured beam size. The emittance terms are shown in Fig.4 for all energies. The origin of the path length in Fig.4 is located at the center of BM1<sub>ss</sub>. The least-squares method was performed to estimate the emittance with the function (1), and results are listed in Fig.4.

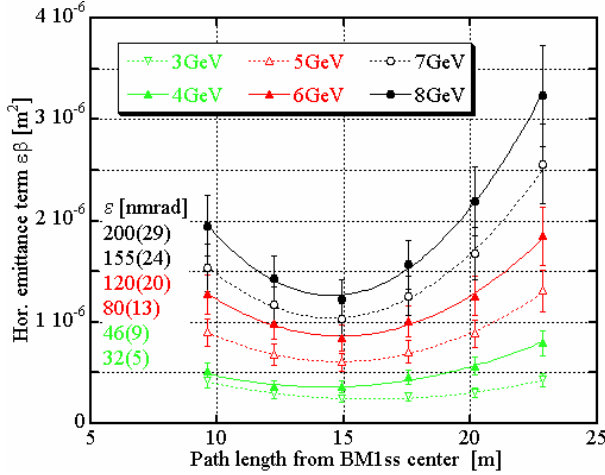


Figure 4: Horizontal emittance terms  $\epsilon\beta$  for various ejected energies. Lines indicate the results of the least-squares method with the function (1). Error bars indicate twice of the error of the beam size. Values of the emittance derived from the least-squares method are also listed. Brackets indicate the error of the fits.

### 5 DISCUSSION

If the emittance growth by the intra-beam scattering is ignored, a natural emittance is expressed as

$$\epsilon_x = C_q \frac{\gamma_E^2}{J_x} \frac{\langle H / \rho^3 \rangle}{\langle 1 / \rho^2 \rangle} \text{ bending-magnet} \quad (4)$$

where,  $C_q$  is the quantum coefficient [m],  $\gamma_E$  is the

$$C_q = \frac{55}{32\sqrt{3}} \frac{\hbar c}{mc^2}, \quad H = \beta\eta^2 + 2\alpha\eta\eta' + \gamma\eta'^2,$$

electron energy over the electron rest energy,  $J_x$  is damping partition number and  $\rho$  is bending radius [m] [5].

The emittance as a function of the energy is shown in Fig.5. The horizontal emittance agreed with the natural emittance within the error of the fit. The emittance growth by the intra-beam scattering was not observed in this energy region. The vertical emittance was obtained from a ratio of the vertical beam size to the horizontal beam size at the position of the OTR7<sub>ss</sub>. It decreased as the energy decreased in the energy range from 5 to 8 GeV, however, increased as energy decreased under 4 GeV.

We presumed this phenomenon as follows. The emittance growth occurred in this energy region. For example, when the acceleration voltage was set to the value for 8 GeV in order to increase an electron density, the emittances at the energy of 3 GeV and 4 GeV

increased approximately 23 times and twice, respectively. In this condition, the amount of increased emittance was 1.3 nmrad at the energy of 3 GeV. In the horizontal direction, the emittance was also increased same order. However, the growth was not observed because the amount was negligibly small compared with the horizontal emittance. As the acceleration voltage was controlled so that the bunch length become shorter in the low energy region in Fig.5, larger emittance growth was observed at lower energy.

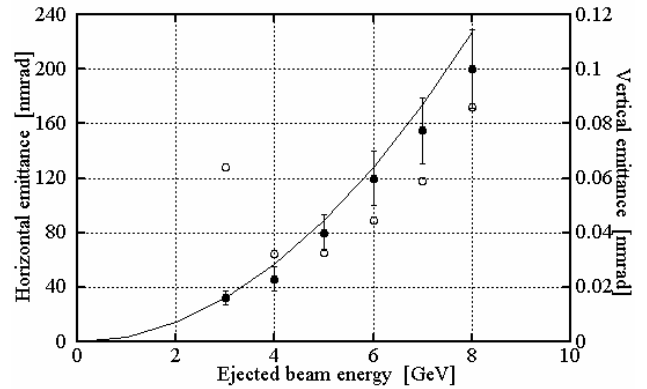


Figure 5: Energy dependence of the emittance. Closed and open circles indicate the horizontal and vertical emittances, respectively. Solid-line indicates the calculated natural emittance in horizontal direction.

### 6 SUMMARY

Energy dependence of the emittance of the ejected beam was measured. The horizontal emittance was proportional to a square of the ejected beam energy at the energy region from 3 GeV to 8 GeV. It was explained by natural emittance due to the quantum excitation. The effect of intra-beam scattering is considered for the vertical emittance growth in the low energy region. We are planning to make precise measurement of the vertical emittance.

### REFERENCES

- [1] K. Fukami et al., "Beam orbit, tune and chromaticity in the SPring-8 booster synchrotron", EPAC2000, Vienna, June 2000.
- [2] T. Okugi et al., "Evaluation of extremely small horizontal emittance", Phys. Rev. Special Topics, Vol.2, 1999.
- [3] M.-A. Tordeux and J. Papadacci, "A new OTR based beam emittance monitor for the linac of LURE", EPAC2000, Vienna, June 2000.
- [4] L. Wartski et al., "Thin films on linac beams as non-destructive devices for particle beam intensity, profile, centering and energy monitors", IEEE Trans., Vol.NS-22, No.3, June 1975.
- [5] H. Wiedemann, "Particle Accelerator Physics", Springer-Verlag, Berlin 1993.